ISSN 2635-1676, Nanobiotechnology Reports, 2021, Vol. 16, No. 6, pp. 732–736. © Pleiades Publishing, Ltd., 2021.
Russian Text © The Author(s), 2021, published in Rossiiskie Nanotekhnologii, 2021, Vol. 16, No. 6, pp. 761–766.

NANOELECTRONICS AND NEUROMORPHIC COMPUTER SYSTEMS

Temporal Coding of Binary Patterns for Learning of Spiking Neuromorphic Systems Based on Nanocomposite Memristors

K. E. Nikiruy[a,*], A. V. Emelyanov[a], A. V. Sitnikov[a], V. V. Rylkov[a,b], and V. A. Demin[a]

[a] *National Research Center Kurchatov Institute, Moscow, Russia*

[b] *Fryazino Branch, Kotelnikov Institute of Radio Engineering and Electronics, Fryazino, 141190 Russia*

**e-mail: NikiruyKristina@gmail.com*

Received July 2, 2021; revised August 3, 2021; accepted August 3, 2021

Abstract—The metal/nanocomposite/metal (M/NC/M) memristive structures based on $(Co_{40}Fe_{40}B_{20})_x(LiNbO_3)_{100-x}$ have been studied. It has been shown that such memristors may change their conductance according to the bioinspired spike-timing-dependent plasticity (STDP) rules. Spiking neural network with 4 presynaptic inputs connected by memristor-synapses with a postsynaptic threshold neuron-integrator has been created, in which the images clustering with temporal coding has been implemented using the STDP rule. Thus, the fundamental possibility of using a temporal coding method, which is more effective than population-frequency coding, has been demonstrated for self-learning of spiking neuromorphic systems with synaptic weights based on nanocomposite memristors.

DOI: 10.1134/S2635167621060161

INTRODUCTION

Computing systems based on the von Neumann architecture successfully cope with most modern problems with deterministic solution algorithms; however, their use in solving poorly defined cognitive problems (pattern recognition, text and speech processing, forecasting, planning, control, etc.) is energy consuming and almost always not optimal from the computational speed point of view [1]. In this regard, neuromorphic computing systems based on memristors that emulate synaptic contacts between artificial neurons can be much more productive and energy efficient [2, 3]. In particular, promising results have recently been demonstrated in the implementation of artificial neural networks based on memristive synapses, such as perceptrons [4, 5], short-term and long-term memory [6], reservoir systems [7] and pulsed neural networks with a simple architecture [8, 9]. Of interest are also experiments on dopamine-like modulation of the resistive state of memristive synapses [10], the possibility of optical monitoring of their condition [11] or work on the observation of the effects of resistive switching of second-order memristors, an analogue of which is also observed for biological synapses [12].

In the case of so-called formal neural networks, the accuracy of their work critically depends on the available volume of data labeled by experts for learning and the number of layers in the multilayer architecture, which limits the range of tasks to be solved (by the presence of appropriate learning samples) and reduces the energy efficiency and computation speed of a system already trained [13].

Recent studies of memristor spiking neuromorphic systems (SNS) showed that when they are trained using biosimilar algorithms, for example, according to the rules of spike-timing-dependent plasticity (STDP), it is possible to significantly reduce the dependence of the pattern classification accuracy on the variability of memristor characteristics [14–16]. Moreover, the use of this rule when learning SNS facilitates the self-adaptation of memristors, the weights of which, in the case of fixed input and output pulse sequences, do not depend on their initial states, but are determined only by information encoded in the delays between pulses [17–19]. Despite the great potential, the computing capabilities of SNS have not been widely demonstrated, especially in comparison with formal networks, primarily due to the lack of effective learning algorithms [20].

To train a SNS according to STDP rules, the most promising approaches are population frequency or temporal coding of information [21]. In frequency coding, the average frequencies of the firing of neurons (generation of impulses or spikes) are used within a selected small time window (a multidimensional image is encoded by a population of such neurons); when coding with a time shift (temporal coding), the signal magnitude is considered higher, the closer the exact moments of generation of presynaptic spikes to the event of pulse generation by the postsynaptic neuron (or vice versa) [22]. Encoding the analog value of

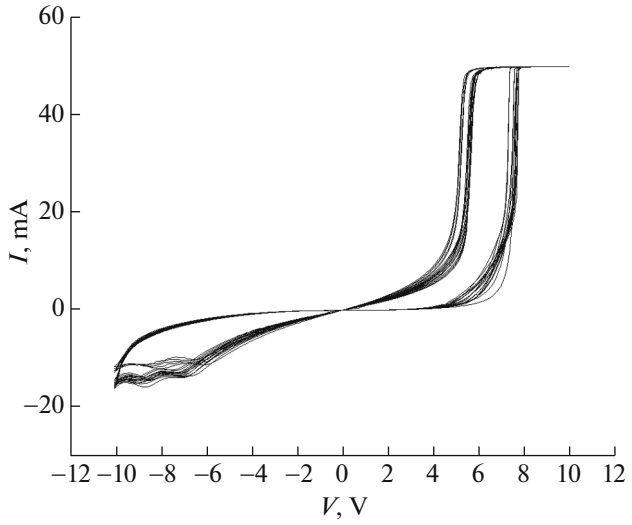

Fig. 1. $I-V$ characteristics of four memristors used to build a pulsed neuromorphic network.

the input signal through the firing rate of the neuron, as a rule, requires a rather large number of spikes, which reduces the energy efficiency and computational performance of the network compared to single pulses in each presynaptic channel for the time-shift coding method. [23]. In addition, with temporal coding, a significantly larger number of signal combinations in the form of spatial-temporal patterns can be recognized by the postsynaptic neuron than in the case of frequency coding, which leads to a significantly greater information capacity of the temporal means of representing information. In these respects, coding information with a time shift looks like a more promising approach [22, 24].

In [19, 24, 25], the possibility of frequency-coded learning of a SNS based on nanocomposite (NC) memristors with a NC of the form $(Co_{40}Fe_{40}B_{20})_x(LiNbO_3)_{100-x}$ has been demonstrated. It has been revealed that SNS learning is possible with a rate ratio of 10:1, and long-term memory can be supported by a low-frequency signal even in the case of using memristors with a finite holding time of their resistive state. The purpose of this work is to study the possibility and peculiarities of learning a SNS based on NC memristors with the temporal coding of information.

EXPERIMENTAL

We used metal/nanocomposite/metal (M/NC/M) memristive structures of the capacitor type based on the NC $(Co_{40}Fe_{40}B_{20})_x(LiNbO_3)_{100-x}$ ($x \approx 10$ at %) synthesized by the method of ion-beam sputtering of a composite target on sitall substrates [26]. The composite was deposited onto substrates previously coated with a Cr/Cu/Cr metal film acting as the bottom contact. The upper contact pads were applied through a metal mask with an aperture size of 0.5 × 0.2 mm.

Electrophysical studies of the M/NC/M structures were carried out using a PXIe-4140 four-channel source meter (National Instruments) at the PM5 analytical probe station (Cascade Microtech). Current–voltage ($I-V$) characteristics were obtained with a grounded bottom electrode and a bias voltage sweep U of the upper electrode linearly in sequence from $0 \rightarrow +U_0 \rightarrow 0 \rightarrow -U_0 \rightarrow 0$ with a step of 0.1 V and a duration of 50 ms, $U_0 = 10$ V.

To test the possibility of changing the weights (conductances) of NC memristive structures according to STDP rules, the lower contact of the structure was used as the presynaptic input, and the upper contact was used as the postsynaptic one (in this case, the potential was measured relative to the lower electrode). Measurements of the conductivity were carried out before and after the application of spikes (voltage pulses of a special shape).

To study the possibility of using a temporal coding scheme for binary images in learning SNS with memristive connections, a simple network was built, consisting of four presynaptic neurons and one postsynaptic threshold neuron connected by NC memristive synapses. The neurons were programmed using a PXIe-4140 source meter in the LabView environment.

RESULTS AND DISCUSSION

It was previously found that memristive structures based on the NC $(Co_{40}Fe_{40}B_{20})_x(LiNbO_3)_{100-x}$ possess resistive switching (RS) with a large ratio of resistances in the low- and high-conductivity states (>100), the number of switching events $>10^6$ and the number of intermediate states $>2^8$ [3, 27]. Under the conditions of resistive switching, a hysteresis is observed in the $I-V$ characteristic (Fig. 1), which is smooth, indicating the relatively weak role of stochastic processes in the RS effect. We associate the latter with the multifilamentary character of the RS caused by the granular nature of the NC, the presence in it of a large number of dispersed Co and Fe atoms (up to $\sim 10^{22}$ cm^{-3}) and self-organized formation of a high-resistance interlayer (~10 nm) of pure (no metal impurities) amorphous $LiNbO_3$ near the lower electrode of the structure during sample synthesis [28]. During the first RS cycles, dispersed atoms nucleate around the percolation chains of CoFe nanogranules, which leads to the formation of metallized filamentary nanochannels connecting the upper electrode of the M/NC/M structure with the amorphous $LiNbO_3$ interlayer determining its resistance. The number of nanochannels and the depth of their penetration into the amorphous $LiNbO_3$ interlayer fully control the general

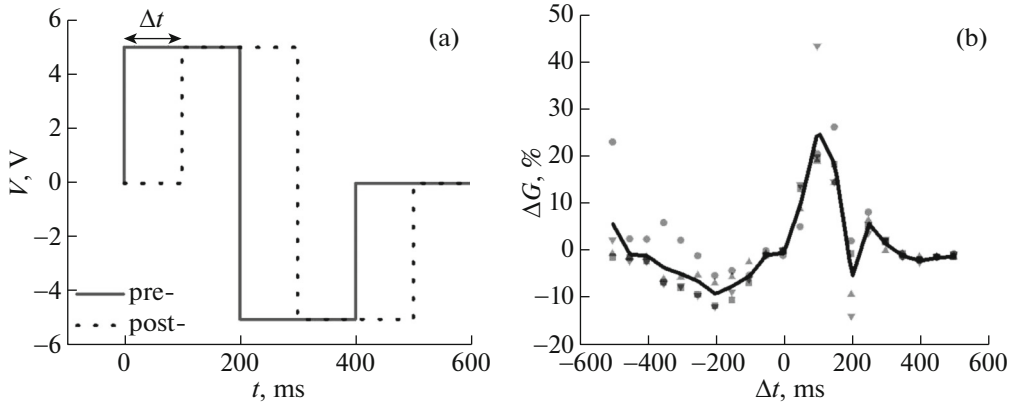

Fig. 2. Presynaptic and postsynaptic voltage pulses (spikes) (a). STDP window: dependence of the change in conductivity on the interspike interval for four memristors (symbols) and average value (solid line) (b).

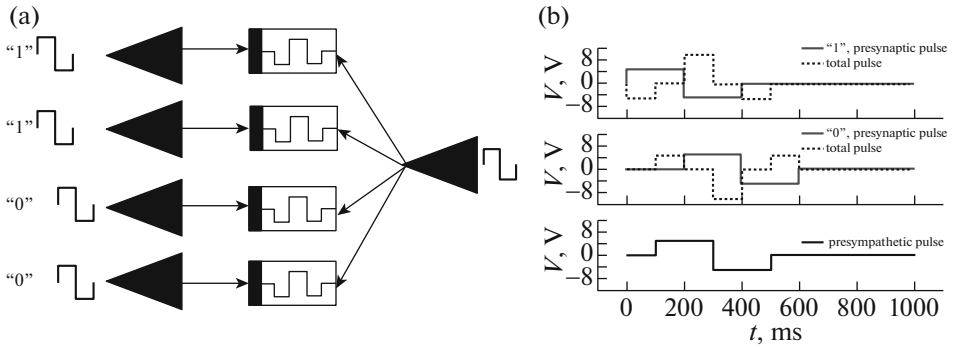

Fig. 3. Scheme of a pulsed neuromorphic network (a) and the spike time sweep (b).

resistive state of the structure, which ensures a high stability and multilevel character of the RS.

An advantage of NC memristors is the ability to change their conductivity quasi-continuously in a wide window [28], also with a possibility to follow STDP rules [9]. In the experiments with STDP, the same presynaptic and postsynaptic spikes were used, which were paired heteropolar rectangular pulses with the same amplitude of 5 V and a duration of 400 ms (Fig. 2a). The change in the relative conductivity (ΔG) depends on the interspike interval (Δt): with a small delay between them, the potential difference across the memristor turns out to be sufficient to change its conductivity. Moreover, if the presynaptic spike occurs earlier than the postsynaptic one ($\Delta t > 0$), an increase in the conductivity (potentiation) is observed, in the opposite case ($\Delta t < 0$), a decrease in the memristor conductivity (depression) is observed (Fig. 2b). A similar relationship is observed for biological synapses [29]. The possibility of the hardware implementation of STDP on M/NC/M memristive structures determines their use as synaptic connections in a SNS.

Using the results obtained, the operability of a simple SNS with temporal coding of the input signal was tested, which consisted of four presynaptic neurons and a postsynaptic threshold integrator neuron without leakage, connected by NC memristive synapses (Fig. 3a). The inputs were sequentially supplied with various binary images consisting of logical "1" and "0". Image coding was implemented by shifting the moment of spike supply from the beginning of the learning cycle. For logical "1", the spike was applied at the beginning of the cycle, and for logical "0", after 200 ms with a total period of one cycle of 1 s (Fig. 3b). Due to the change in the time of the onset of the presynaptic impulse, the resulting voltage on the memristor during the generation of the postsynaptic spike is positive for "1" (corresponds to $\Delta t > 0$) and negative for "0" (corresponds to $\Delta t < 0$). After 100 such learning cycles, the conductance ratio for four different images was ~10, after 500 s, it was about two (Fig. 4). A decrease in the ratio of the conductivity values occurs due to the relaxation of the resistive state after exposure to electrical pulses (Fig. 5). The relaxation time characterizing the duration of retention of the resistive state was ~50 s for the used memristive elements. In this case, for a low-conductivity state, after a sharp increase in conductivity, its gradual decrease is

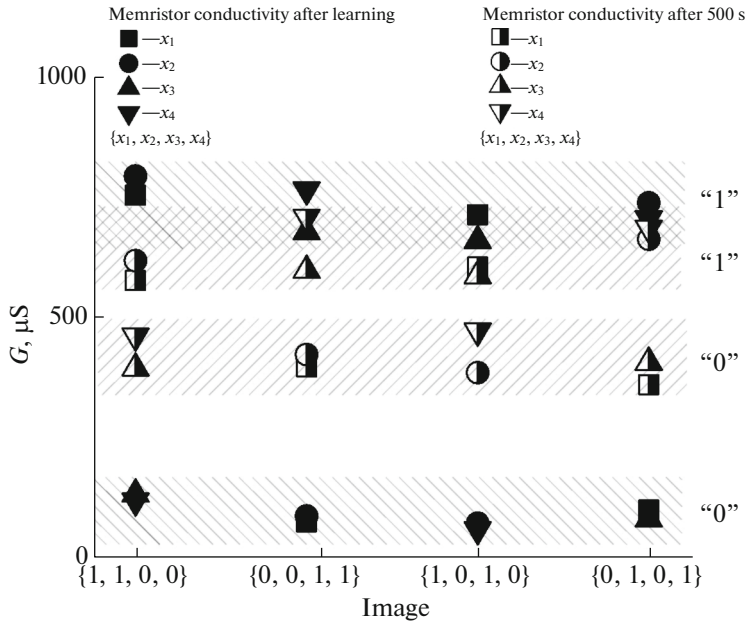

Fig. 4. Result of learning the spiking neuromorphic network immediately after 100 learning cycles and after 500 s.

observed, as a result of which the ratio of conductivities increases (Fig. 5). Figure 4 shows that the final state of the system unambiguously corresponds to the images supplied to the presynaptic inputs.

In contrast to works [17–19, 30–32], which demonstrate learning based on STDP rules, this paper shows the possibility of learning a hardware SNS with temporal coding of an image. We note that for unambiguous interpretation of the results obtained, binary images were used, although learning can also be carried out to recognize a pattern from analog signals using a suitable STDP window shape. Indeed, a continuous change in the conductivity corresponding to a given pattern occurs depending on the interspike interval that arises between the input and output pulses, while the magnitude of the change is directly determined by the shape and amplitude of the curve in the STDP window, which in turn depends on the spike parameters. When using spikes of a different shape (bitriangular, sawtooth, sinusoidal), the STDP window does not qualitatively change [10], and therefore, learning SNS with temporal coding can be expected for other forms of spikes.

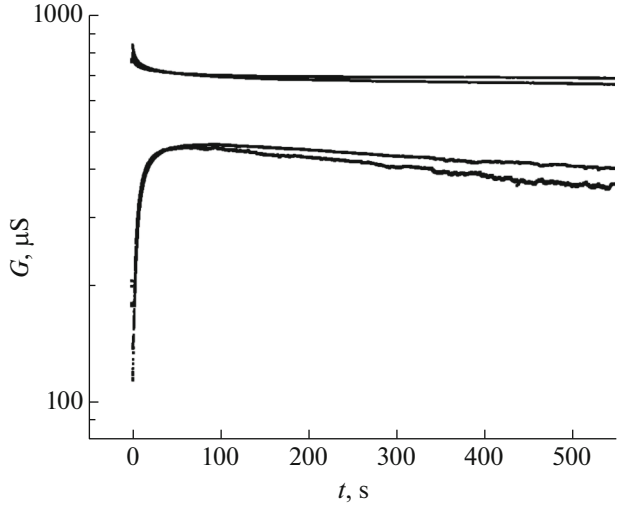

Fig. 5. Change in the conductivity of four memristors depending on the time after learning the pulsed neuromorphic network.

CONCLUSIONS

It is shown that it is possible to solve the problem of clustering binary images encoded by the time-shift method by a simple pulsed neuromorphic system with synaptic connections based on NC memristors with an active layer of the form $(Co_{40}Fe_{40}B_{20})_x(LiNbO_3)_{100-x}$ ($x \approx 10$ at %). After 100 learning cycles, the conductivity ratio for four different images was ~10, after 500 s, at least two were stable (taking into account the relaxation of the resistive states of the memristors). This determines the fundamental suitability of memristive NC structures and systems based on them for self-learning of pattern recognition with the temporal coding of information, along with the previously demonstrated possibility of learning SNS with nanocomposite memristive weights of clustering population-frequency patterns. Thus, in future studies, systems based on NC memristors with hybrid information-coding methods can be built, which expands the prospects for

their use in the development of universal neuromorphic computing systems.

ACKNOWLEDGMENTS

The studies were carried out using equipment of the resource center for electrophysical methods (National Research Center "Kurchatov Institute").

FUNDING

This work was partially supported by a grant from the President of the Russian Federation (MK-2203.2021.1.2) in terms of studying the electrophysical properties of memristor samples and by the Russian Science Foundation (grant no. 18-79-10253) in terms of learning a spiking neuromorphic network with temporal-coded signals.

REFERENCES

1. K. Berggren, Q. Xia, K. K. Likharev, et al., Nanotechnology **32**, 012002 (2021). https://doi.org/10.1088/1361-6528/aba70f
2. S. Shchanikov, A. Zuev, I. Bordanov, et al., Chaos Solitons Fractals **142**, 110504 (2021). https://doi.org/10.1016/j.chaos.2020.110504
3. V. V. Rylkov, A. V. Emelyanov, S. N. Nikolaev, K. E. Nikiruy, A. V. Sitnikov, E. A. Fadeev, V. A. Demin, and A. B. Granovsky, J. Exp. Theor. Phys. **131**, 160 (2020). https://doi.org/10.1134/S1063776120070109
4. M. Prezioso, F. Merrikh-Bayat, B. D. Hoskins, et al., Nature (London, U.K.) **521**, 61 (2015). https://doi.org/10.1038/nature14441
5. A. V. Emelyanov, D. A. Lapkin, V. A. Demin, et al., AIP Adv. **6**, 111301 (2016). https://doi.org/10.1063/1.4966257
6. C. Li, Z. Wang, M. Rao, et al., Nat. Mach. Intell. **1**, 49 (2019). https://doi.org/10.1038/s42256-018-0001-4
7. J. Moon, W. Ma, J. H. Shin, et al., Nat. Electron. **2**, 480 (2019). https://doi.org/10.1038/s41928-019-0313-3
8. A. D. Pisarev, A. N. Busygin, S. Y. Udovichenko, et al., Microelectron. J. **102**, 104827 (2020). https://doi.org/10.1016/j.mejo.2020.104827
9. N. V. Andreeva, E. A. Ryndin, and M. I. Gerasimova, BioNanoSci. **10**, 824 (2020). https://doi.org/10.1007/s12668-020-00778-210
10. K. E. Nikiruy, I. A. Surazhevsky, V. A. Demin, et al., Phys. Status Solidi A **217**, 1900938 (2020). https://doi.org/10.1002/pssa.201900938
11. D. A. Lapkin, A. N. Korovin, S. N. Malakhov, et al., Adv. Electron. Mater. **6** (10), 1 (2020). https://doi.org/10.1002/aelm.202000511
12. A. N. Matsukatova, A. V. Emelyanov, A. A. Minnekhanov, et al., Appl. Phys. Lett. **117**, 243501 (2020). https://doi.org/10.1063/5.0030069
13. Y. Zhang, Z. Wang, J. Zhu, et al., Appl. Phys. Rev. **7**, 011308 (2020). https://doi.org/10.1063/1.5124027
14. D. Querlioz, O. Bichler, P. Dollfus, et al., IEEE Trans. Nanotechnol. **12**, 288 (2013). https://doi.org/10.1109/TNANO.2013.2250995
15. S. Brivio, D. Conti, M. V. Nair, et al., Nanotechnology **30**, 015102 (2019). https://doi.org/10.1088/1361-6528/aae81c
16. V. A. Demin, D. V. Nekhaev, I. A. Surazhevsky, et al., Neural Netw. **134**, 64 (2021). https://doi.org/10.1016/j.neunet.2020.11.005
17. M. Prezioso, M. R. Mahmoodi, F. Merrikh-Bayat, et al., Nat. Commun. **9**, 5311 (2018). https://doi.org/10.1038/s41467-018-07757-y
18. K. E. Nikiruy, A. V. Emelyanov, V. V. Rylkov, A. V. Sitnikov, and V. A. Demin, Tech. Phys. Lett. **45**, 386 (2019). https://doi.org/10.1134/S1063785019040278
19. A. V. Emelyanov, K. E. Nikiruy, A. V. Serenko, et al., Nanotechnology **31**, 045201 (2020). https://doi.org/10.1088/1361-6528/ab4a6d
20. Q. Xia and J. J. Yang, Nat. Mater. **18**, 309 (2019). https://doi.org/10.1038/s41563-019-0291-x
21. A. Sboev, A. Serenko, R. Rybka, et al., Math. Methods Appl. Sci., **1** (2020). https://doi.org/10.1002/mma.6241
22. C. Stockl and W. Maass, Nat. Mach. Intell. **3**, 230 (2021). https://doi.org/10.1038/s42256-021-00311-4
23. A. Sboev, D. Vlasov, R. Rybka, et al., Proc. Comput. Sci. **145**, 458 (2018). https://doi.org/10.1016/j.procs.2018.11.107
24. I. A. Surazhevsky, V. A. Demin, A. I. Ilyasov, et al., Chaos Solitons Fractals **146**, 110890 (2021). https://doi.org/10.1016/j.chaos.2021.110890
25. A. I. Iliasov, A. V. Emelyanov, K. E. Nikiruy, et al., Tech. Phys. Lett. (2021). https://doi.org/10.1134/S1063785021070075
26. V. V. Rylkov, S. N. Nikolaev, V. A. Demin, A. V. Emelyanov, A. V. Sitnikov, K. E. Nikiruy, V. A. Levanov, M. Yu. Presnyakov, A. N. Taldenkov, A. L. Vasiliev, K. Yu. Chernoglazov, A. S. Vedeneev, Yu. E. Kalinin, A. B. Granovsky, V. V. Tugushev, and A. S. Bugaev, J. Exp. Theor. Phys. **126**, 353 (2018). https://doi.org/10.1134/S1063776118020152
27. K. E. Nikiruy, A. V. Emelyanov, V. A. Demin, et al., AIP Adv. **9**, 065116 (2019). https://doi.org/10.1063/1.5111083
28. M. N. Martyshov, A. V. Emelyanov, V. A. Demin, et al., Phys. Rev. Appl. **14**, 034016 (2020). https://doi.org/10.1103/PhysRevApplied.14.034016
29. G. Hennequin, E. J. Agnes, and T. P. Vogels, Ann. Rev. Neurosci. **40**, 557 (2017). https://doi.org/10.1146/annurev-neuro-072116-031005
30. E. Covi, R. George, J. Frascaroli, et al., J. Phys. D: Appl. Phys. **51**, 34003 (2018). https://doi.org/10.1088/1361-6463/aad361
31. A. Serb, J. Bill, A. Khiat, et al., Nat. Commun. **7**, 12611 (2016). https://doi.org/10.1038/ncomms12611
32. Z. Wang, S. Joshi, S. Savel'ev, et al., Nat. Electron. **1**, 137 (2018). https://doi.org/10.1038/s41928-018-0023-2